Proc. of the 5th WSEAS/IASME Int. Conf. on Electric Power Systems, High Voltages, Electric Machines, Tenerife, Spain, December 16-18, 2005 (pp46-51)

A Robust and Adaptive RBF Neural Network Based on Sliding Mode Controller for Interior Permanent Magnet Synchronous Motors

MEHRAN RASHIDI
Faculty of Engineering, Hormozgan University, Bandar-Abbas
IRAN

Abstract – Electric motors play an important role in consumer and manufacturing industries. Among all different kinds of electric motors, Interior Permanent Magnet Synchronous Motors (IPMSM) have a special place. That is because of their high torque to current ratio, large power to weight ratio, high efficiency, high power factor and robustness. In this paper a radial basis function (RBF) neural network based on sliding mode controller (SMC) is presented to control IPMSM. A RBF neural network is formulated as a controller whose parameters must be updated. To guarantee the robustness of the closed-loop system, a modified SMC methodology is designed to derive an adaptation law for the parameters of neural network controller. The weights of the neural network can be adaptively adjusted for the compensation of uncertain dynamics and the tracking error between the plant output and the model output can be guaranteed to converge to zero in a finite time. The effectiveness of the proposed control system is verified by some simulations results. Obtained results show the response time is also very fast despite the fact that the control strategy is based on bounded rationality.

Key-Words: Speed Control, IPMSM, Disturbance, Nonlinear model, RBF neural network, Sliding mode control

1 Introduction

The advances in power semiconductor technology, digital electronics, magnetic materials and control theory have enabled modern ac motor drives to face challenging high efficiency and high performance requirements in the industrial sector. Among ac drives, the permanent magnet synchronous motor has been gaining popularity owing to its high torque to current ratio, large power to weight ratio, high efficiency, high power factor and robustness. These features are due to the incorporation of high energy rare-earth alloys such as Neodymium-Iron-Boron in its construction. Especially, the interior permanent magnet synchronous motor (IPMSM) which has magnets buried in the rotor core exhibit certain good properties, such as, mechanically robust rotor construction, a rotor non-saliency and low effective air gap. The rotors of these machines have a complex geometry to ensure optimal use of the expensive permanent magnet material while maintaining a high magnetic field in the air gap. These features allow the IPMSM drive to be operated in high-speed mode by the field weakening. Usually high performance motor drives require fast and accurate response, quick recovery from any disturbances and insensitivity to parameter variations. The dynamic behavior of an ac motor can be significantly improved using vector control theory where motor variables are transformed into an orthogonal set of d-q axes such that speed and torque can be controlled separately [1]. This gives the IPMSM machine the highly desirable dynamic performance capabilities of the separately excited dc machine, while retaining the general advantages of the ac over dc motors. Originally, vector control was applied to the induction motor and a vast amount of research work has been devoted to this area. The vector control method is relevant to IPMSM drive as the control is completely carried out through the stator as the rotor excitation control is not possible. However, precise speed control of an IPMSM drive becomes a complex issue owing to nonlinear coupling among its winding currents and the rotor speed as well as the nonlinearity present in the torque equation. The system nonlinearity becomes severe if the IPMSM drive operates in the field weakening region where the direct axis current $i_d \neq 0$. This results in the appearance of a non-linear term, which would have vanished under the existing vector control scheme with $i_d = 0$. There have been significant developments in nonlinear control theory applicable to electric motor drives. Interestingly, the d-q transformation applicable to ac motors can be considered as a feedback linearization transformation. However, with the recent developments in nonlinear control theories, a modern control engineer has not only found a systematic approach in dealing with nonlinearities but has managed to develop approaches, which had not been considered previously. The surges of such nonlinear control methods applicable to electromechanical systems include variable structure systems [2], differential geometric approach [3], [4] and passivity theory [5]. However, most of these controllers are complex to implement or take a lot of cost, so it is important problem to design controller that require least cost with good performance. This paper focuses on solving these complex control problems via an innovative approach: use of RBF based on Sliding mode control. This paper is organized as follows. Firstly, the IPMSM drive model in the d-q reference frame is presented in Section 2. Then in Section 3 the structure of proposed radial basis function (RBF) neural network based on sliding mode controller (SMC) is presented. The block diagram of control system and its blocks are described in Section 4 and simulation results are presented in Section 5. Finally, the conclusion is presented in Section 6.

2. The IPMSM Model

The mathematical model of an IPMSM drive can be described by the following equations in a synchronously rotating rotor d-q reference frame as [6]:

$$\begin{bmatrix} vd \\ vq \end{bmatrix} = \begin{bmatrix} R + pL_d & -Pw_r L_q \\ Pw_r L_d & R + pL_q \end{bmatrix} \begin{bmatrix} i_d \\ i_q \end{bmatrix} + \begin{bmatrix} 0 \\ Pw_r \Psi_f \end{bmatrix} \quad \textbf{(1)}$$

$$T_e = T_L + J_m p w_r + B_m w_r \quad \textbf{(2)}$$

$$T_e = \frac{3P}{2}[\Psi_f i_q + (L_d - L_q) i_d i_q] \quad \textbf{(3)}$$

It is well known that a synchronous motor is unable to self-start when supplied with a constant frequency source. The starting torque in the IPMSM drive used in our research is provided by a rotor squirrel cage winding. The starting process of the IPMSM drive can be considered as a superposition of two operating modes, namely, unsymmetric asynchronous motor mode and magnet-excited synchronous generator mode [7]. Therefore, the effects of shorted rotor windings have to be considered, if one wants to examine the process of run-up to the synchronization. However, the model equations in (1) to (3) do not describe the asynchronous behavior of the IPMSM drive. The IPMSM drives constructed using Neodymium-Iron-Boron magnets can be operated over a wide temperature orange [8]. It has been shown that, within normal operating temperature range, the residual flux density and intrinsic coercivity will decrease as the temperature is increased. However, this is considered as a reversible process as the temperature comes down to normal value, the flux density and coercivity will return to their original values. This variation in residual flux along with the stator resistance, in turn affects the dynamic behavior of the motor controller. The standard linear d-q axis IPMSM model with constant parameters will lead to an unsatisfactory prediction of the performance of a permanent-magnet motor owing to the extraordinary saturation of these machines during normal operation. It has been shown that improved prediction of IPMSM behavior can be accomplished by adjusting the model parameters according to the changing saturating conditions [9]. Various researchers have proved that here exists variations in *Xd, Xq* , and Ψ_f. with the direct and quadratic axis saturation as well as with the direction of rotation [7,9]. In light of these findings we propose to use BELBIC controller wherein this controller response all of this variation in system. The objective of this paper is to obtain the IPMSM control voltages in order to achieve high performance speed tracking. According to the motor model given in equations (1-3) of section II, it can be seen that the speed control can be achieved by controlling the q-axis component v_q of the supply voltage as long as the d-axis current i_d *is* maintained at zero. This results in the electromagnetic torque being directly proportional to the current i_q . Since $i_d = 0$, the d-axis flux linkage depends only on the rotor permanent magnets. The resultant IPMSM model can be represented as,

$$pi_d = \frac{1}{L_d}(v_q - Ri_q - Pw_r \Psi_f) \quad \textbf{(4)}$$

$$v_d = -w_r L_q i_q \quad \textbf{(5)}$$

$$T_e = T_L + J_m p w_r + B_m w_r \quad \textbf{(6)}$$

$$T_e = \frac{3P}{2}(\Psi_f i_q) \quad \textbf{(7)}$$

3. Proposed Controller Formation

Consider the following single-input single-output nonlinear dynamical system:

$$\begin{aligned} x^{(n)} &= f(x, \dot{x}, \ldots, x^{(n-1)}, u) = f(X(t), u) \\ y(t) &= x(t) \end{aligned} \quad \textbf{(8)}$$

Where $X(t) = [x, \dot{x}, \ldots, x^{(n-1)}]$ denotes the state of system, u and y represent the control input and the system is output respectively, and $f(.)$ is a multi-input single-output nonlinear function. We assume that

$$0 < \frac{\partial f}{\partial u} < B_{f_u} \quad \textbf{(9)}$$

We define

$$R(t) = \left[r(t), \dot{r}(t), \ldots, r^{(n-1)}(t) \right] \quad \textbf{(10)}$$

Where $r(t)$ is the desired system output whose n^{th} derivative is assumed to exit. We can define error vector $E(t)$ as:

$$E(t) = X(t) - R(t) \quad \textbf{(11)}$$

To track the desired output, a radial basis function neural network (RBFNN) controller in the form of:

$$u(E) = \sum_{i=1}^{N_h + 1} w_i(t) \phi_i(E(t)) \quad \textbf{(12)}$$

Is used as the controller where

$$\begin{aligned} \phi_i(E(t)) &= \phi_i\left(\frac{\|E(t) - c_i\|}{\sigma_i}\right), \qquad i = 1, 2, \ldots, N_h \\ \phi_{N_h+1}(E(t)) &= 1 \end{aligned} \quad \textbf{(13)}$$

and $E(t)$ is the input of radial basis function, N_h is the number of radial basis functions (i.e., the number of hidden neurons), c_i is the center of the ith radial basis function $\varphi_i(.), \sigma_i$ is proportional to the effective radius of the ith basis function and w_i is the connection weight between the hidden neuron i and the output layer. There is no connection weight between the input layer and the hidden layer. Typically, $\phi_i(.)$ is a Gaussian function in the form of:

$$\phi_i(x) = \exp\left(-\frac{\|x - c_i\|^2}{2\sigma_i^2}\right) \quad \textbf{(14)}$$

Re-writing Equation (5) in vector form yields:

$$u(E) = W^T(t)\Phi(E(t)) \quad \textbf{(15)}$$

The overall system with the controller is shown in Figure 1.

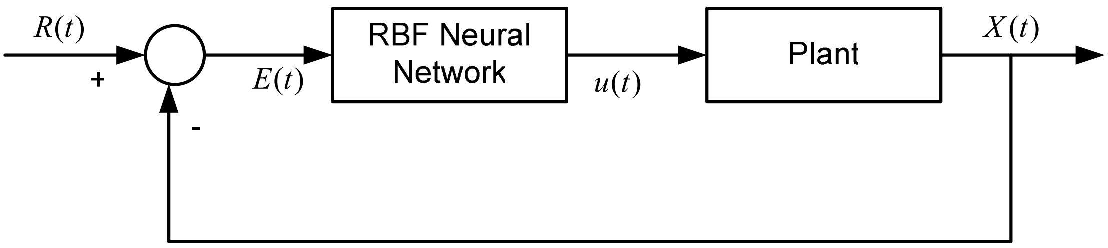

Fig.1. Structure of the control system

Without loss of generality, we impose the following constraints to the neural network controller [10]:

$$\|W(t)\| = \sqrt{\sum_{i=1}^{N_h} w_i(t)^2} \leq B_W \quad \textbf{(16)}$$

$$\|\Phi(t)\| = \sqrt{\sum_{i=1}^{N_h} \phi_i(t)^2} \leq B_\phi \quad \textbf{(17)}$$

3. Sliding Mode-Based Adaptation Law for RBFNN Controller

In this section we will present an update law for the controller parameters using the sliding mode and then we will show the stability of the resulting control law by Lyapunov theorem. Consider a sliding surface in the form of:

$$s(t) = e(t) + k_1\dot{e}(t) + \dots + k_n e^{(n)}(t) \quad \textbf{(18)}$$

Where

$$e(t) = y(t) - r(t) \quad \textbf{(19)}$$

With defining:

$$\begin{aligned} r_1(t) &= r(t) + k_1\dot{r}(t) + \dots + k_n r^{(n)}(t), \\ x_1(t) &= x(t) + k_1\dot{x}(t) + \dots + k_{n-2}x^{(n-2)}(t) \end{aligned} \quad \textbf{(20)}$$

In addition, according to equation (8), we can re-write the sliding surface in equation (19) as a following form:

$$s(t) = x_1(t) - r_1(t) + k_{n-1}x^{(n-1)}(t) + k_n f(X(t), u) \quad \textbf{(21)}$$

For the system given in Equation (8) with radial basis function neural network controller given in (12), let:

$$W(t) = \frac{\Phi(t)}{\Phi^T(t)\Phi(t)k_n \dfrac{\partial f}{\partial u}}\left[-k\Psi(s(t)) - u_1(t)\right] \quad \textbf{(22)}$$

Where

$$u_1(t) = \dot{r}_1(t) + \dot{x}_1(t) + k_{(n-1)}f(X(t), u) + k_n \sum_{i=0}^{n-1} \frac{\partial f}{\partial x^i} x^{(i+1)} \quad \textbf{(23)}$$

And

$$\Psi(s) = \gamma sign(s) + (1 - \gamma)\tanh(\alpha s) \quad \textbf{(24)}$$

The constant parameters α and γ are chosen such that $\alpha > 0, 0 < \gamma < 1$ and k is a sufficiently large constant satisfying:

$$k > \frac{k_n B_W B_\Phi B_{f_u}}{\gamma} \quad \textbf{(25)}$$

Then, the adaptation mechanism defined in (22) enforces the controller parameters $w_i(t)$ to the values that lead the states of the system to the sliding surface defined in (18) by driving an arbitrary initial values of *s(t)* to zeros.

Proof: Consider following preliminaries. From Equation (24), we have:

$$\arg\min_x \{\|\Psi(x)\|\} = \gamma \quad \textbf{(26)}$$

With respect to (21) the derivative of *s(t)* is written as follow:

$$\begin{aligned}&\dot{s}(t) = -\dot{r}_1(t) + \dot{x}_1(t) + k_{n-1} f\big(X(t), u\big) + \\ &k_n \sum_{i=0}^{n-1} \frac{\partial f}{\partial x^i} x^{(i+1)} + k_n \frac{\partial f}{\partial u} \dot{u} \\ &u_1(t) + k_n \frac{\partial f}{\partial u} \dot{u}\end{aligned} \quad \textbf{(27)}$$

Also, form (13) we have:

$$\Phi^T(t)\Phi(t) = 1 + \sum_{i=1}^{N_h} (\phi_i(E(t)))^2 > 0 \quad \textbf{(28)}$$

At last, rewriting Equation (22) we get:

$$k_n \frac{\partial f}{\partial u} \Phi^T(t)\Phi(t)\dot{W}^T(t) = \Phi^T(t)\big[-k\Psi(s(t)) - u_1(t)\big] \quad \textbf{(29)}$$

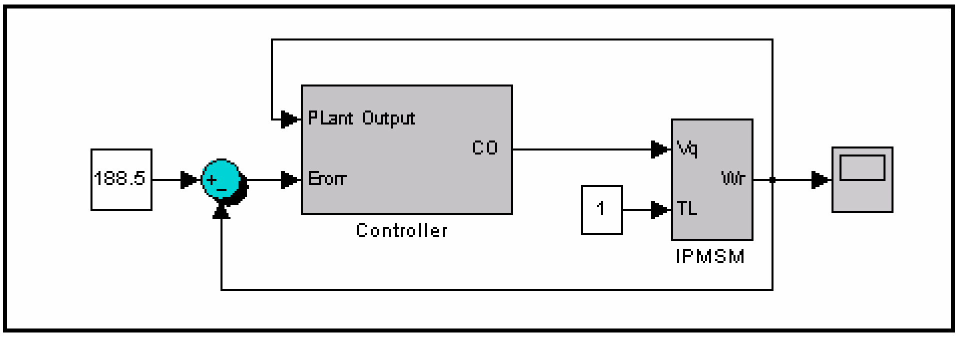

Fig. 2. The Control system structure

Multiplying both sides by $\Phi(t)$ follows that:

$$\begin{aligned}&k_n \frac{\partial f}{\partial u} \Phi^T(t)\Phi(t)\dot{W}^T(t)\Phi(t) = \\ &\Phi^T(t)\Phi(t)\big[-k\Psi(s(t)) - u_1(t)\big]\end{aligned} \quad \textbf{(30)}$$

Dividing both sides by $\Phi^T(t)\Phi(t)$ yields:

$$k_n \frac{\partial f}{\partial u} \dot{W}^T(t)\Phi(t) + u_1(t) = -k\Psi(s(t)) \quad \textbf{(31)}$$

Now, Consider a Lyapunov function candidate of the form:

$$V(s(t)) = \frac{1}{2} s(t)^2 \quad \textbf{(32)}$$

Using Equation (20), the derivative of $V(s(t))$ with respect to time is given by:

$$\dot{V}(s(t)) = s(t)\dot{s}(t) = s(t)\left[u_1(t) + k_n \frac{\partial f}{\partial u} \dot{u}\right] \quad \textbf{(33)}$$

Substituting the derivative of Equation (8) into above equation yields:

$$\dot{V}(s(t)) = s(t)\left[\begin{aligned}&u_1(t) + k_n \frac{\partial f}{\partial u} \dot{W}^T(t) \times \\ &\Phi(t) + k_n \frac{\partial f}{\partial u} W^T(t)\dot{\Phi}(t)\end{aligned}\right] \quad \textbf{(34)}$$

Using Equations (24) and (27) and inequality (2), (9), and (10), we have:

$$\begin{aligned}&\dot{V}(s(t)) = s(t)\left[-k\Psi(s(t) + k_n \frac{\partial f}{\partial u} W^T(t)\dot{\Phi}(t)\right] \le \\ &\le |s(t)|\big[k_n B_{f_u} B_W B_\Phi - k|\Psi(s(t))|\big] \le \\ &\le |s(t)|\big[k_n B_{f_u} B_W B_\Phi - k \min\{|\Psi(s(t))|\}\big]\end{aligned} \quad \textbf{(35)}$$

Finally, applying Equation (19) and using Equation (18), we get:

$$\dot{V}(s(t)) \le |s(t)|\big[k_n B_{f_u} B_W B_\Phi - k\gamma\big] \le 0 \quad \textbf{(36)}$$

Therefore, the controlled trajectory of the error asymptotically converges to zero. In adjusting the parameter of neural network, we must have $\frac{\partial f}{\partial u}$ and $\frac{\partial f}{\partial x^i}$. However, when the system is unknown, we must model the function f off-line using another neural network and use $\frac{\partial \hat{f}}{\partial u}$ and $\frac{\partial \hat{f}}{\partial x^i}$ in place of $\frac{\partial f}{\partial u}$ and $\frac{\partial f}{\partial x^i}$ respectively where $\hat{f}$ is the neural network model of the function f.

4. The Block Diagram of the Control System

The control method for the IPMSM is chosen based on some parameters including: usage, performance and speed range.

Figure2 shows the block diagram of the control system.

5. Simulation Results

In order to validate this controller and hence, to establish the effectiveness of the proposed controller, the performance of the IPMSM drive based on the proposed control scheme is investigated at different operating conditions. Sample results are presented below. Digital simulations have been carried out using MATLAB/SIMULINK. The parameters of the laboratory IPMSM drive are given in Table I. In figure 3 there is investigated the tracking of system, In this case the drive system is started at a constant load of 1N m with the speed reference set at 1800 r/min (188.5 rad/sec). It can be seen from Figure 3 that the actual speed converges to the reference value within 0.1 s. However, according to this figure the stator current shows an overshoot but it lasts for only 0.08 s. Another simulated speed response for a sudden increase in command speed is shown in Figure 4 .It is evident from this figure that proposed method is also capable of handling the disturbance in speed command. For investigating the performance of system in spite of disturbance, load is changed 3N.m at 0.5 sec, The simulation result of this condition are shown in figure 5, The actual speed does not change during the disturbance while the stator current swiftly reaches to its new value corresponding to the load applied. This shows the capability of new controller in terms of disturbance rejection. Computer simulations have been carried out to determine system responses for an industry standard proportional-integral-derivative (PID)-controlled. Obtained results showed that although steady-state error of the speed is quite low, the overall performance is inferior to that of the proposed controller.

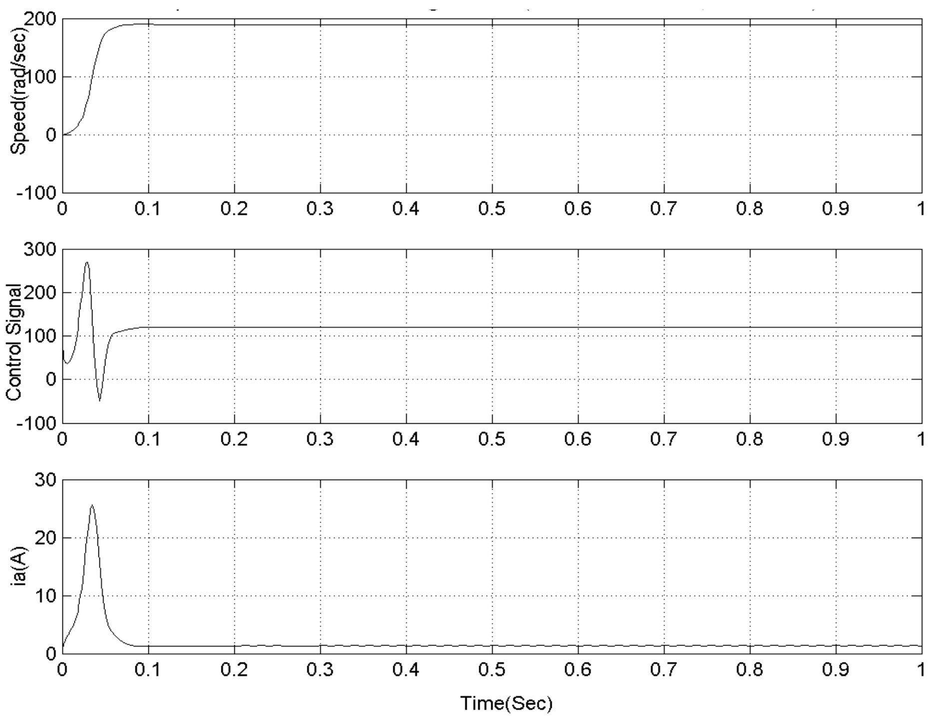

Fig. 3. Speed control of PMSM using Proposed Controller

Conclusion

In this paper a novel approach for control of IPMSM was discussed. The method was based on RBF neural network that to guarantee the robustness of the closed-loop system, a modified SMC methodology was designed to derive an adaptation law for the adjust parameters of neural controller. By adding the n^{th} order error derivative term to the sliding surface, we were able to incorporate the approximation information of the plant (i.e., the plant neural model) in the adaptation mechanism. Using a Lyapunov-Based adaptation law, the tracking error vector was driven to the sliding manifold with smooth control effort. The developed control structure solves the chattering problem without degrading the tracking performance. Online learning, fast convergence, and learning stability were the most important advantages of this controller that were shown in the simulation results. Other important advantage of this method is its robustness and relative independency to plant model that makes it more interesting for real application.

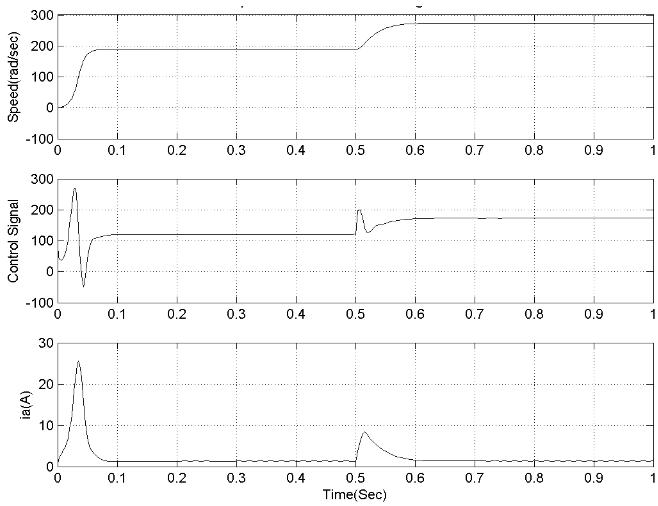

Figure 4.Simulated response for sudden increase in speed for the proposed control system

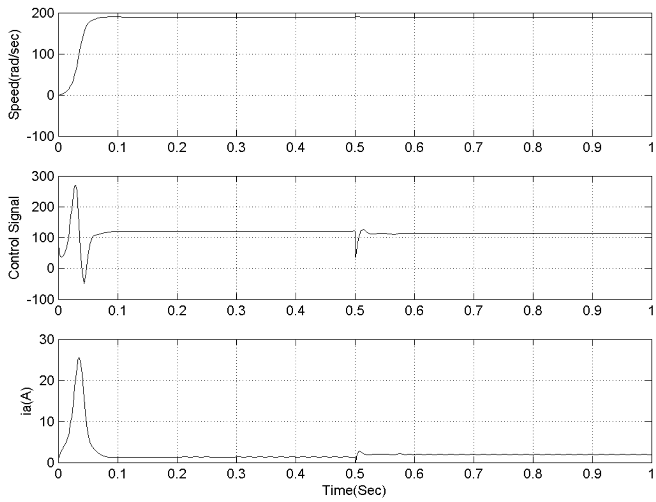

Figure 5.Simulation response for sudden increase in load for the proposed control system

Reference

[1] F. Blaschke, "The principle of field orientation as applied to the new transvector closed-loop control system for rotating-field machines," Siemens Rev., vol. 34, pp. 217–220,(May,1972).

[2] V. Utkin, Sliding Modes in Control Optimization: Springer Verlag, (1992).

[3] R. Marino, S. Peresada, and P. Valigri, "Adaptive input-output linearizing control of induction motors," IEEE Trans. Automat. Control, vol. 38, pp. 208–221, (February, 1993).

[4] M. Ilic-Spong, R. Marino, S. Peresada, and D. Taylor, "Feedback linearizing control of switched reluctance motors," IEEE Transaction. Automatica Control., vol. 32, pp. 371–379,(May,1987)

[5] R. Ortega, P. J. Nicklasson, and G. Espinosa, "Passivity-based control of the general rotating electrical machines," in Proceeding IEEE Conference Decision and Control, pp. 4018–4023 (1994).

[6] T. S. Radwan, M. A. Rahman, A. M. Osheiba, and A. E. Lashine, "Dynamic analysis of a high performance permanent magnet synchronous motor drive," in Pro c. IEEE Canadian Conference Electrical and Compute Engineering, pp. 611–614 (1996).

[7] M. A. Rahman and P. Zhou, "Analysis of brushless permanent magnet synchronous motors," IEEE Transaction Industrial Electronic, vol. 43, pp. 256–267 (April 1996).

[8] T. Sebastian, "Temperature effects on torque production and efficiency of PM motors using NdFeB magnets," IEEE Transaction Industrial. Application, vol. 31, no. 2, pp. 353–357 (March/April 1995).

[9] P. H. Mellor, F. B. Chaaban, and K. J. Binns, "Estimatio n of parameters and performance of rare-earth permanent-magnet motors avoiding measurement of load angle," in Proceeding Inst. Electrical Engineering, vol. 133, pp: 322–330 (November, 1991).

[10] Hunt K. J., Sbarbaro D., Zbikowski R. and Gawthrop P. J. (1992), "Neural networks for control systems - A survey", *Automatica*, 28, pp. 1083-1112.

[11] K. Jezernik, M. Rodic, R. Safaric and B. Curk (1997), "Neural Network Sliding Mode Control," Robotica, Vol. 15, pp. 23-30.

[12] O. Kaynak, M. O. Efe, X. Yu, B. M. Wilamowski (2001), "Sliding Mode Control of Nonlinear Systems Using Gaussian Radial Basis Function Neural Network", IEEE Conference, pp. 474-479.

[13] Y. C. Chang (2001), "Adaptive fuzzy-Based Control for Nonlinear SISO Systems via VSS and H infinity Approach", IEEE Trans. on Fuzzy Systems, vol. 9, No. 2, pp. 278-292.